NeuroImage 172 (2018) 506–516

Contents lists available at ScienceDirect

NeuroImage

journal homepage: www.elsevier.com/locate/neuroimage

A common brain network among state, trait, and pathological anxiety from whole-brain functional connectivity

Yu Takagi [a,b,*], Yuki Sakai [a,c], Yoshinari Abe [c], Seiji Nishida [c], Ben J. Harrison [d], Ignacio Martínez-Zalacaín [e], Carles Soriano-Mas [e,f,g], Jin Narumoto [c], Saori C. Tanaka [a,*]

[a] ATR Brain Information Communication Research Laboratory Group, Kyoto, Japan
[b] Graduate School of Information Science, Nara Institute of Science and Technology, Nara, Japan
[c] Department of Psychiatry, Graduate School of Medical Science, Kyoto Prefectural University of Medicine, Kyoto, Japan
[d] Melbourne Neuropsychiatry Centre, Department of Psychiatry, The University of Melbourne and Melbourne Health, Melbourne, Australia
[e] Department of Psychiatry, Bellvitge Biomedical Research Institute-IDIBELL, Barcelona, Spain
[f] Centro de Investigación Biomédica en Red de Salud Mental (CIBERSAM), Barcelona, Spain
[g] Department of Psychobiology and Methodology of Health Sciences, Universitat Autònoma de Barcelona, Barcelona, Spain

ARTICLE INFO

Keywords:
Functional connectivity fMRI
Dimensional psychiatry
Anxiety
Data-driven approach
Machine learning
Human connectome project

ABSTRACT

Anxiety is one of the most common mental states of humans. Although it drives us to avoid frightening situations and to achieve our goals, it may also impose significant suffering and burden if it becomes extreme. Because we experience anxiety in a variety of forms, previous studies investigated neural substrates of anxiety in a variety of ways. These studies revealed that individuals with high state, trait, or pathological anxiety showed altered neural substrates. However, no studies have directly investigated whether the different dimensions of anxiety share a common neural substrate, despite its theoretical and practical importance. Here, we investigated a brain network of anxiety shared by different dimensions of anxiety in a unified analytical framework using functional magnetic resonance imaging (fMRI). We analyzed different datasets in a single scale, which was defined by an anxiety-related brain network derived from whole brain. We first conducted the anxiety provocation task with healthy participants who tended to feel anxiety related to obsessive-compulsive disorder (OCD) in their daily life. We found a common state anxiety brain network across participants (1585 trials obtained from 10 participants). Then, using the resting-state fMRI in combination with the participants' behavioral trait anxiety scale scores (879 participants from the Human Connectome Project), we demonstrated that trait anxiety shared the same brain network as state anxiety. Furthermore, the brain network between common to state and trait anxiety could detect patients with OCD, which is characterized by pathological anxiety-driven behaviors (174 participants from multi-site datasets). Our findings provide direct evidence that different dimensions of anxiety have a substantial biological inter-relationship. Our results also provide a biologically defined dimension of anxiety, which may promote further investigation of various human characteristics, including psychiatric disorders, from the perspective of anxiety.

Introduction

Anxiety is a future-oriented mental state activated by distant and potential threats rather than specific and predictable ones (Calhoon and Tye, 2015). On the one hand, anxiety drives us to avoid frightening situations and to achieve our goals. On the other hand, excessive anxiety may cause distress and impairment in daily life. Although anxiety is a common mental state in humans, we experience anxiety in a variety of forms. For example, public speaking or leaving one's home can induce anxiety related to a fear of negative evaluation by others and risk of theft, respectively. Such anxieties may drive us to do something to overcome our anxiety, such as practicing a speech or repeatedly checking that the house door is locked.

One conventional way to study anxiety is to investigate the state associated with the feeling of anxiety, namely, state anxiety. Other studies focus on the frequency of anxiousness, namely, trait anxiety, which is measured using self-report questionnaires. Another major research field concerns the anxiety of patients with psychiatric

* Corresponding authors. ATR Brain Information Communication Research Laboratory Group, Kyoto, Japan.
E-mail addresses: yu.takagi@atr.jp (Y. Takagi), xsaori@atr.jp (S.C. Tanaka).

https://doi.org/10.1016/j.neuroimage.2018.01.080
Received 30 June 2017; Received in revised form 27 January 2018; Accepted 30 January 2018
Available online 1 February 2018

disorder. This type of anxiety includes social anxiety disorder, obsessive-compulsive disorder (OCD), and generalized anxiety disorder. Such "pathological anxiety", which is defined by clinically significant levels of anxiety (i.e., excessive, uncontrollable anxiety), incurs tremendous socioeconomic costs (Greenberg et al., 1999) and roughly 30% of people experience an anxiety-related disorder at some point in their lifetime (Kessler et al., 2005).

In the neuroscience field, a large number of studies have investigated the neural substrates of anxiety using functional magnetic resonance imaging (fMRI). For each dimension of anxiety, these studies have used different experimental approaches to investigate neural substrates. To investigate the brain activity underlying state anxiety, researchers have experimentally induced participant's anxiety inside of the MRI scanner (Mataix-Cols et al., 2003; Satpute et al., 2012). Other studies focused on the relationship between trait anxiety and brain activity (Baur et al., 2013; Kim et al., 2011; Modi et al., 2015; Tian et al., 2016; Yin et al., 2016). These latter studies have recently focused on changes in brain activity, measured by resting-state fMRI (rs-fMRI). Finally, other studies have focused on the difference between populations with pathological anxiety and healthy controls. Some studies have found altered brain activation during anxiety provocation tasks, and others have found altered brain networks during resting state or anxiety provocation tasks (Banca et al., 2015; Beucke et al., 2013; Cha et al., 2014; Etkin et al., 2010; Giménez et al., 2012; Hahn et al., 2011; Harrison et al., 2009; Liu et al., 2015; Sakai et al., 2011; Wang et al., 2016).

Previous findings have suggested an interaction among state, trait, and pathological anxiety (e.g., Mathews, 1990; Williams et al., 1996). If there is a common biological substrate, it has the potential to be used for risk assessment and early detection of pathological anxiety, which would enable its evaluation for treatment. From a theoretical perspective, it would also be helpful to understand the dynamics of the development of pathological anxiety. In addition, given that the hypothesis of a psychiatric disorder spectrum is gaining attention (Adam, 2013), such a biologically defined index would provide an objective, reliable biological dimension of anxiety for the spectrum, which may be valuable for understanding various human characteristics, including psychiatric disorders. However, no studies have directly investigated whether there is a common biological substrate among state, trait, and pathological anxiety.

To determine whether there is a common biological substrate among state, trait, and pathological anxiety, we adopted a single neuronal index defined by anxiety-related functional connectivity (FC), a measure of temporally correlated fluctuations in blood oxygen level-dependent (BOLD) signal among different regions. FC has been successfully used to elucidate neural mechanisms of various individual characteristics (Cole et al., 2012; Finn et al., 2015; Liem et al., 2016; Rosenberg et al., 2016). Indeed, FCs have been correlated with individual differences in state or trait anxiety (Baur et al., 2013; Modi et al., 2015; Satpute et al., 2012; Tian et al., 2016) and are different between healthy people and individuals with pathological anxiety (Banca et al., 2015; Beucke et al., 2013; Cha et al., 2014; Etkin et al., 2010; Giménez et al., 2012; Hahn et al., 2011; Harrison et al., 2009; Liao et al., 2010; Liu et al., 2015; Sakai et al., 2011; Wang et al., 2016).

Here, in a data-driven manner, we directly tested the hypothesis that there is a common brain network among state, trait, and pathological anxiety. We first investigated whether state and trait anxiety shared a common brain network in healthy people. Then, to investigate how state and trait anxiety are involved in pathological anxiety, we tested which sets of FCs were generalized to patients with OCD, a disorder characterized by pathological anxiety-driven behavior, among the brain networks related to state and/or trait anxiety.

Materials and methods

Anxiety provocation task

Participant recruitment

To effectively extract anxiety-related brain networks, we recruited 10 healthy participants (9 men, ages 20–24 years, mean age 22.2 years) who tended to be anxious in their daily life from 432 volunteers who completed a questionnaire prior to the fMRI experiments. Specifically, we recruited participants who had a score of greater than or equal to 80 on the Padua Inventory (Burns et al., 1996) or 13 on the Maudsley Obsessional Compulsive Inventory (Hodgson and Rachman, 1977). All participants were primarily evaluated using the Structured Clinical Interview for DSM-IV Axis I Disorders-Non-Patient Edition (SCID-NP) (First et al., 2002). No participant had a current DSM-IV Axis I diagnosis of any significant psychiatric disorder. Participant consent was obtained in accordance with a protocol reviewed and approved by the Ethics Committee of the Advanced Telecommunications Research Institute International. At the time of the experiments, the mean ± standard deviation of the Padua Inventory and Maudsley Obsessional Compulsive Inventory were 71.5 ± 23.6 and 13.2 ± 2.3, respectively.

Stimuli selection

Previous studies demonstrated that neural activity related to anxiety can be extracted using fMRI by presenting two sets of stimuli to participants (Blair et al., 2008; Giménez et al., 2012; Lorberbaum et al., 2004; Mataix-Cols et al., 2003; Rotge et al., 2008; Tillfors et al., 2001)One set of stimuli is for provoking anxiety (anxiety stimuli), for example, the image of a key hole, which may induce anxiety about theft. The other set of stimuli is a relatively neutral stimulus, for example, the image of a nature scene. Here, we conducted a similar task, by iteratively presenting two sets of stimuli to the participants while controlling the semantics (categories of the objects) and basic features (color and luminance) of the two sets of stimuli (Fig. 1a; see Supplementary Notes). Before the fMRI experiments, all participants rated their subjective anxiety in response to approximately 200 images in a Likert scale between 1 and 9 (rate 1 for lowest anxiety and 9 highest anxiety among all images). Then, for each participant, anxiety images, those with the top 50 rating scales, and neutral images, those with the bottom 50 rating scales, were selected as stimuli for the fMRI.

Experimental paradigm

Seven participants attended 6 MRI scanner sessions and 3 participants attended 12 sessions. Each session consisted of 4 blocks, an anxiety block or a neutral block, and each block consisted of 6 trials. The block type order was randomized for all participants. In the first trial of each block, a cue was presented on the screen for 1 s ("anxiety" in the anxiety block, "neutral" in the neutral block). Twenty stimuli were then presented at a rate of 200 ms per stimulus, to minimize the effects of the basic feature and semantic content of a particular stimulus, and was followed by a 14-s imagination period, during which participants were instructed to be anxious if they were in the anxiety block or to relax if they were in the neutral block. After the imagination period, participants were asked to rate their level of anxiety on a 4-point Likert scale (rate 1 for "no anxiety" and 4 for "very anxious"). A fixation cross was superimposed on each stimulus, and participants were instructed to maintain fixation on this cross throughout the scanning session. For each session, in two randomly selected trials, participants needed to push the button in response to the change in fixation color on the display to guarantee that participants maintained fixation. These trials were excluded from the subsequent analysis.

fMRI procedure

A 3-T Siemens Trio scanner (Erlangen, Germany) with a 12-channel head coil was used to perform T2*-weighted echo planar imaging (EPI). We acquired 275 scans for each session with a gradient echo EPI

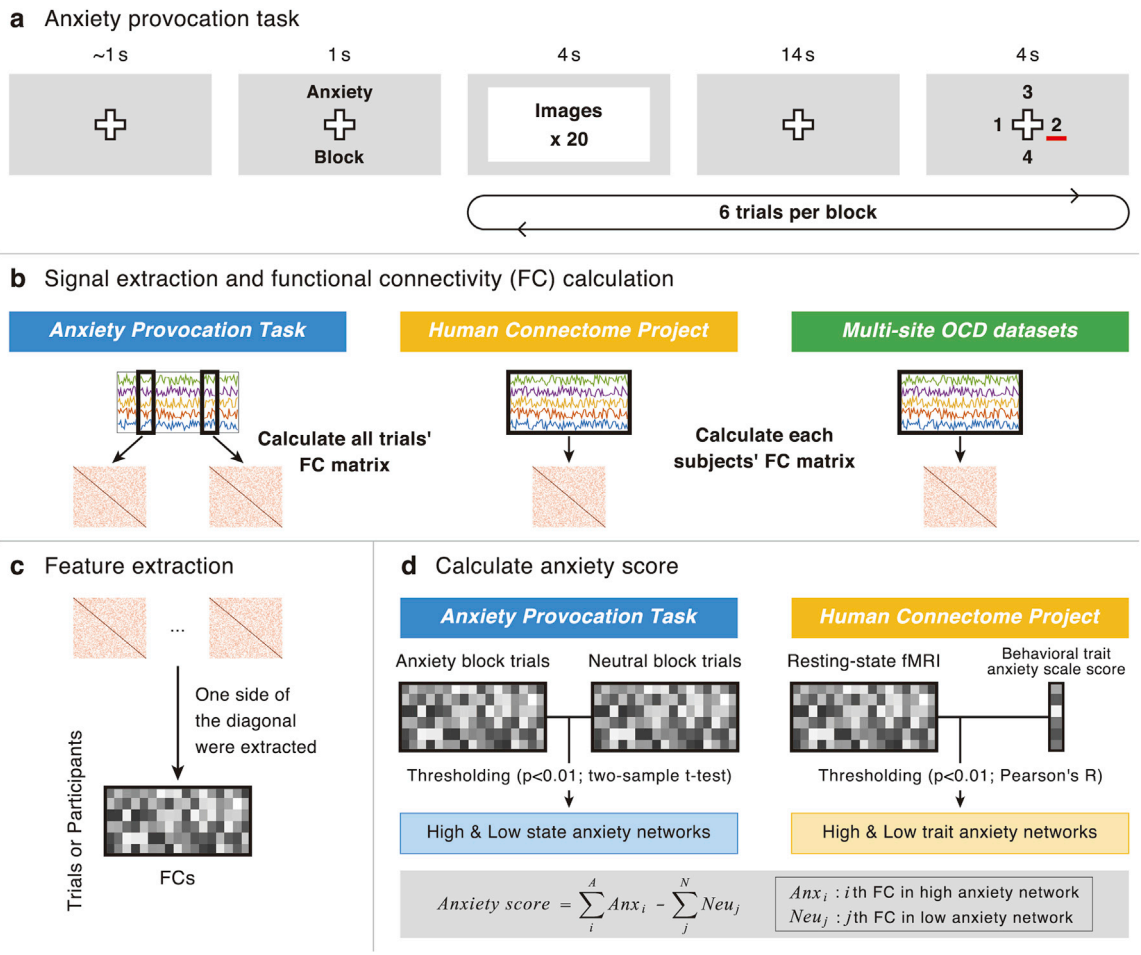

Fig. 1. Experimental paradigm and definition of anxiety score. (a) The sequence of events for a given trial of the anxiety provocation task. **(b–d)** Schematic diagram of the analyses. (**b**) Three types of datasets were used, that is, anxiety provocation task, Human Connectome Project, and multi-site OCD datasets. Signals of interest were extracted from all participants. The signals were then turned into functional connectivity (FC) via covariance estimation. Note that trial-wise FC matrices were estimated for the anxiety provocation task. In contrast, participant-wise FC matrices were estimated for the Human Connectome Project dataset and multi-site OCD datasets. (**c**) FC matrices were turned into the feature matrix for the subsequent analysis. (**d**) FCs with a strong relationship to anxiety were selected via statistical thresholding through cross-validation. Anxiety scores for trials/participants were calculated by summing FCs in the high-anxiety network and summing sign-inversed FCs in the low-anxiety network.

sequence. The first 7 scans were discarded to allow for T1 equilibration. The following scanning parameters were used: repetition time (TR), 2000 ms; echo time (TE), 30 ms; flip angle (FA), 80°; field of view (FOV), 192 × 192 mm; matrix, 64 × 64; 33 oblique slices tilted to the anterior commissure–posterior commissure line (Deichmann et al., 2003); and a 3.5-mm slice thickness without gap. Although some ROIs suffered from signal omission in the parietal areas because of the oblique acquisition, there was no signal omission in the amygdala. T1-weighted anatomical imaging with an MP-RAGE sequence was performed with the following parameters: TR, 2250 ms; TE, 3.06 ms; FA, 9°; FOV, 256 × 256 mm; matrix, 256 × 256; 208 axial slices; and slice thickness, 1 mm without gap.

Preprocessing

We used Statistical Parametric Mapping 8 (SPM8: Wellcome Department of Cognitive Neurology, http://www.fil.ion.ucl.ac.uk/spm/software/) in MATLAB for preprocessing and statistical analyses. The raw functional (EPI) images were initially corrected for slice-timing and realigned to the mean image of that sequence to compensate for head motion. Structural (T1) images were then co-registered to the mean functional image and segmented into three tissue classes in Montreal Neurological Institute (MNI) space. Using the associated parameters, the functional images were then normalized and resampled in a $2 \times 2 \times 2\,mm^3$ grid. Finally, they were smoothed by a Gaussian full-width at half-maximum of 6 mm. To avoid the effects of motion artifacts, we employed the "scrubbing" procedure to identify and exclude any frames exhibiting excessive head motions (Power et al., 2012) (see Supplementary Notes for detail).

Interregional correlation analysis

For each participant, a pair-wise, interregional FC was evaluated among 268 regions of interest (ROIs) covering the entire brain (Finn et al., 2015). We extracted the representative time course in each region by averaging the time courses of the voxels therein. The time courses were bandpass filtered (0.045–0.18 Hz) (Gonzalez-Castillo et al., 2015) and then linearly regressed by the temporal fluctuations in white matter, cerebrospinal fluid, and entire brain, as well as six head motion parameters. We determined the fluctuation in each type of tissue from the average time course of the voxels within a mask created by the segmentation procedure of the T1 image. The mask for the white matter was eroded by one voxel to consider a partial volume effect. These extracted time courses were bandpass filtered (0.045–0.18 Hz) before the linear regression, as was performed for the regional time courses (Gonzalez-Castillo et al., 2015). We defined 10 scans, offset 4 s from the stimulus onset (to account for the delay in hemodynamic response), as the trial scans. For each participant, a matrix of the FCs of each trial between all

ROIs was then calculated using scans belonging to each trial by evaluating pair-wise temporal Pearson correlations of BOLD time courses (Fig. 1b). Because FC matrices are symmetric, values on only one side of the diagonal were kept, resulting in 35,778 unique FCs ($268 \times 267/2$) for each trial (Fig. 1c). A final trial in each session has not enough trial scans defined above, that is 10 scans offset 4s from the stimulus onset. Therefore, we excluded the trial from subsequent analysis.

Within-participant anxiety detection

To test the hypothesis that there is a common brain network of anxiety within participants, we first investigated the difference in FCs between trials in different blocks (i.e., the anxiety and neutral blocks) in a fully cross-validated manner (Fig. 2a) for each participant. Cross-validation tests the ability of the model to generalize and involves separating the data into subsets. We analyzed all datasets in a single scale, which was defined by the FCs and named an "anxiety score" (Fig. 1d) (Shen et al., 2017). The score is defined by a subset of the data (the "training" set), and then the generalizability of the score is tested in the fully independent remainder of the data (the "test" set). Here, we conducted 10-fold cross-validation, that is, we split all trials into 10 sets of trials for each participant. For each FC, we then conducted a two-sample *t*-test between the mean values of FC of anxiety and neutral trials using the all but one held-out test set. The resulting *P* values were statistically thresholded at $P < 0.01$ and separated into a positive tail (FC tends to be higher during provocation [anxiety] blocks) and a negative tail (FC tends to be higher during neutral blocks). We named these FCs high- and low-anxiety networks, respectively. Finally, to validate whether our model reliably detects anxiety in the test set, anxiety scores for trials in the test set were calculated by summing FCs in the high-anxiety network and summing the sign-inversed FCs in the low-anxiety network. Note that, although we term this a "within-participant" analysis, there was no exact paired relationship between the neutral trials and anxiety trials. Therefore, we conducted two-sample *t*-tests, rather than paired *t*-tests.

Across-participant generalization

As an additional step, we investigated whether the FCs selected from other participants could be generalized to held-out participants. In other words, we tested whether there was a common brain network of state anxiety across participants. To investigate this, we expanded the previous analysis from the within-participant paradigm to the across-participant paradigm (Fig. 2b). Specifically, for each participant, we calculated the anxiety scores of all trials using almost the same procedure as described in the previous section. However, here, we defined the anxiety score by the other participants' trials. Thus, we conducted analyses in a leave-one-participant-out cross-validation manner. Note that when we extracted high- and low-anxiety networks from more than one participant, we also conducted a two-way repeated measures analysis of variance (ANOVA) that considered participant as a factor (participant × stimulus [anxiety or neutral]). This analysis confirmed our results and shows that they do not depend on the method of feature selection (see Supplementary Notes for detailed results).

Resting-state fMRI: Human Connectome Project

To investigate whether there is a common brain network between state and trait anxiety in healthy people, we tested whether the anxiety score defined by state anxiety can be generalized to rs-fMRI with the behavioral trait anxiety scale score.

Participants and behavioral measure

We used a public rs-fMRI dataset from the Human Connectome Project (HCP) 900 Subject Release (Van Essen et al., 2012). These data were acquired using a protocol with advanced multiband rs-fMRI sequences for 15 min. The datasets were preprocessed through the common preprocessing pipeline of the HCP (Griffanti et al., 2014; Salimi-Khorshidi et al., 2014). We also conducted scrubbing procedure as we described above for the anxiety provocation task. As a behavioral trait anxiety measure, the NIH Toolbox Fear-Affect Survey, which is a computerized adaptive test comprising items from the PROMIS Anxiety Item Bank (Pilkonis et al., 2011), was used. Participants with both rs-fMRI and behavioral measures were included in the subsequent analyses. The final set of participants comprised 879 participants. More details on these data are described in the Supplementary Notes.

Beyond anxiety dimension generalization

For each participant in the HCP data, using the same ROIs used in the analysis for the state anxiety, the representative time course in each region was extracted by averaging the time courses of the voxels therein. For each participant, a matrix of FC between all ROIs was then calculated using scans by evaluating pair-wise temporal Pearson correlations of BOLD signal time courses of whole scans (Fig. 1b and c). We then extracted the FCs related to behavioral trait anxiety scale score by calculating Pearson correlations between all FCs and participants' behavioral measure of trait anxiety (Fig. 1d). Similar to the analyses for the state anxiety alone, the resulting *P* values were statistically thresholded at $P < 0.01$ and separated into a positive tail (a higher FC value means that the participant was more likely to have a high behavioral trait

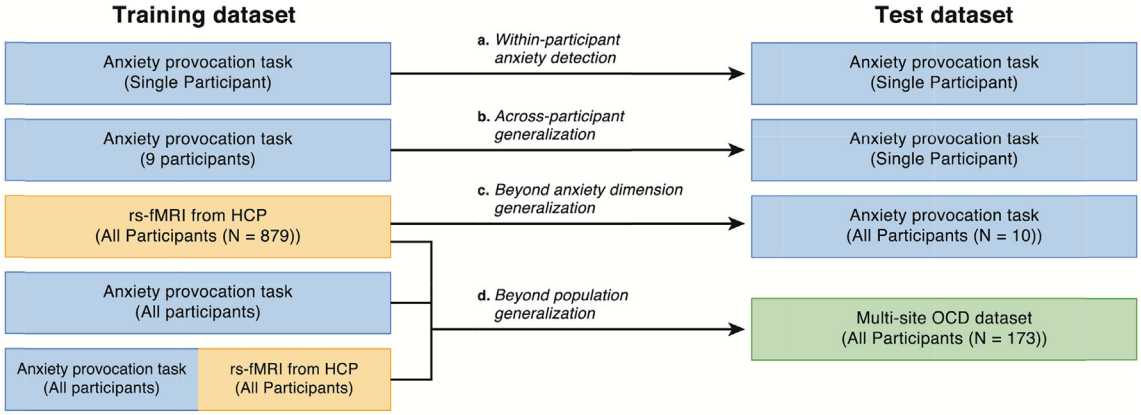

Fig. 2. Schematic diagram of the analyses. Anxiety scores were defined by the training dataset and generalized to the held-out test dataset. **(a)** Within-participant anxiety detection was conducted in a 10-fold cross-validation manner. **(b)** Across-participant generalization was conducted in a leave-one-participant-out cross-validation manner. **(c)** Beyond anxiety dimension generalization was conducted using the anxiety score that was defined by the HCP data. **(d)** Beyond population generalization was conducted using anxiety scores defined by the FCs related to state and/or trait anxiety. We also conducted leave-one-participant-out classification within multi-site OCD datasets.

anxiety scale score) and a negative tail (a higher FC value means that the participant was more likely to have a low behavioral trait anxiety scale score). Again, we called these FCs high- and low-anxiety networks, respectively. The anxiety score was calculated for all participants' trials in the anxiety provocation task, as previously described (Fig. 2c).

Common brain network between state and trait anxiety

To evaluate the degree of overlap between sets of FCs related to state and trait anxiety, we then tested whether the number of common FCs was significantly higher than chance. The FC was considered to be common if it was included in the same network (high- or low-anxiety network) of both state and trait anxiety. Note that the FCs related to state anxiety were defined by FCs that were selected at all iterations through the leave-one-participant-out cross-validation procedure for the anxiety provocation task. The FCs related to trait anxiety were defined by FCs that were selected using the HCP data. To determine the number of common FCs obtained by chance, we compared randomly created networks of state and trait anxiety. First, we shuffled the trial labels of the anxiety provocation task and defined a high- and low-state anxiety network as described in the previous section. We then also shuffled the behavioral trait anxiety scale scores of the HCP data and defined a high- and low-trait anxiety network. We ran these analyses 10,000 times and defined 10,000 random high- and low-anxiety networks for both the state and trait data. Finally, we calculated the number of common FCs between state and trait anxiety for every random high- and low-anxiety network.

Prediction of patients with OCD

Even if there is a set of FCs related to state and/or trait anxiety in healthy people, the relationships between these networks and pathological anxiety is still a question that remains to be directly investigated. Therefore, we asked which set of FCs is altered in the population with pathological anxiety among the FCs related to state and/or trait anxiety. To investigate this question, we used three rs-fMRI datasets consisting of two different populations, namely, healthy controls (HCs) and patients with OCD, which is characterized by pathological anxiety-driven behavior.

Participants

We recruited participants at three different sites: sites A and B in Japan and site C in Spain. Supplementary Table 1 shows a summary of the participants' demographic information. Each imaging site adopted its own imaging protocol (Supplementary Table 2), differing in imaging parameters. The complete recruitment criteria are described in the Supplementary Notes.

At site A (Kajiicho Medical Imaging Center, Kyoto, Japan), the same dataset used by Takagi et al. (2017) was used. All resting-state fMRI data (56 OCD and 52 HCs) were collected at Kajiicho Medical Imaging Center, Kyoto, Japan. The Medical Committee on Human Studies at Kyoto Prefectural University of Medicine, Kyoto, Japan, approved all of the procedures in this study. All participants gave written informed consent after receiving a complete description of the study. For each participant, a single 6-min 40-s continuous resting functional scan and a high-resolution T1-weighted anatomical image were acquired.

At site B (KPUM), the same dataset used by Sakai et al. (2011) was used. Because 15 participants were also included in site A, we excluded them from site B. Finally, 28 participants were included (10 OCD and 18 HCs). The Medical Committee on Human Studies at Kyoto Prefectural University of Medicine, Kyoto, Japan, approved all of the procedures in this study. All participants gave written informed consent after receiving a complete description of the study. For each participant, a single 8-min continuous resting functional scan and a high-resolution T1-weighted anatomical image were acquired.

At site C (Bellvitge University Hospital, Barcelona, Spain), the same dataset reported by Harrison et al. (2009) was included. Forty-two participants were recruited from the Department of Psychiatry, Bellvitge University Hospital, Barcelona, Spain. Because data were not available on 4 of the 21 HCs, we excluded them from our analysis. Finally, 21 patients with OCD and 17 HCs were included in the dataset. All participants gave written informed consent after receiving a complete description of the study. The institutional review board of the Bellvitge University Hospital, Barcelona, approved all of the procedures in this study. For each participant, a single 4-min continuous resting functional scan and a high-resolution T1-weighted anatomical image were acquired.

Preprocessing

We used SPM8 for preprocessing and statistical analyses in a similar manner to our previous rs-fMRI studies (Takagi et al., 2017). Raw functional images were first corrected for slice-timing and realigned to the mean image of that sequence to compensate for head motion. Structural images were then co-registered to the mean functional image and segmented into three tissue classes in the MNI space. Using associated parameters, the functional images were then normalized and resampled in a $2 \times 2 \times 2\,mm^3$ grid. Finally, they were smoothed by a Gaussian full-width at half-maximum of 6 mm. We also conducted scrubbing procedure as we described above for the anxiety provocation task and HCP data. A bandpass filter (0.008–0.1 Hz) was then applied to the sets of time courses. The filtered time courses were linearly regressed by the temporal fluctuations of the white matter, cerebrospinal fluid, and entire brain, as well as six head motion parameters. These extracted time courses were bandpass filtered (0.008–0.1 Hz) before the linear regression, as was performed for regional time courses. Finally, for each participant, using the same ROIs and procedure for the rs-fMRI from the HCP data, the rs-FC matrix was calculated (Fig. 1b and c). The complete procedure is described in the Supplementary Notes.

Beyond population generalization

To investigate how state and trait anxiety are involved in pathological anxiety, we tested which sets of FCs were generalized to patients with OCD, among the brain networks related to state and/or trait anxiety. That is, we calculated three types of the anxiety score for each participant in the multi-site OCD datasets. Their anxiety scores were calculated by summing the FCs in the high-anxiety network and summing the sign-inversed FCs in the low-anxiety network (Fig. 1d). These networks were defined by state and/or trait anxiety data (Fig. 2d). We then compared the anxiety scores of HCs with those of patients with OCD or state and/or trait anxiety.

Machine-learning classification

Recently, rs-fMRI has received attention as a biomarker of psychiatric disorder in the clinical field (Fox and Greicius, 2010). Therefore, we tested whether the selected high- and low-anxiety networks could also be generalized to the population with OCD. Note that, although several studies have investigated neurological biomarkers of OCD (Gruner et al., 2014; Hu et al., 2016; Li et al., 2014; Soriano-Mas et al., 2007; Takagi et al., 2017; Weygandt et al., 2012), our study is distinct because we did not use any diagnostic label and focused on the dimensions of the anxiety. In other words, our main motivation was not to construct an optimal biomarker for the clinical usage but to investigate common FCs' characteristics as a scientific finding. We conducted the classification via leave-one-participant-out cross-validation employing a sparse logistic regression classifier (Yamashita et al., 2008). Thus, the weights of the classifier were estimated using training participants and were validated using test participants. For this analysis, we used the common FCs between state and trait anxiety because only this set of FCs was generalized to pathological anxiety in the previous analysis (see the Results). Furthermore, to demonstrate that the results cannot be reproduced by randomly selected FCs, we picked the same number of FCs randomly from all 35,778 FCs and then conducted the same procedure 10,000 times to determine the distribution of the area under the curve (AUC).

Interpretation of anxiety-related FC patterns

To facilitate characterization of the biological substrates of the anxiety-related brain network, we summarized the FC patterns that were obtained from the state anxiety, trait anxiety, and their overlap. We grouped the 268 ROIs into eight macroscale canonical networks (e.g., the default mode network) and examined the number of FCs between each pair of regions in each network; these canonical networks were defined functionally in a previous study (Finn et al., 2015).

Results

State anxiety-related network: anxiety provocation task

Within-participant anxiety detection

To test whether there is a brain network that is consistently different between neutral and anxious states within participants, we compared the anxiety scores of the trials in different blocks in a cross-validated manner for each participant (Fig. 2a). We tested whether the anxiety scores of trials in the neutral block were lower than those of trials in the anxiety block. We applied a two-way repeated measures ANOVA to the anxiety scores of all trials (N = 1,585; participant × stimulus [anxiety or neutral]) and identified a significant effect of stimulus ($F_{(1,1584)} = 191.54$; $P = 3.51 \times 10^{-41}$). Fig. 3a shows the anxiety scores of the anxiety and neutral trials, which were normalized within each participant. We also found a significant effect of participant ($F_{(9,1584)} = 85.47$; $P = 3.28 \times 10^{-129}$) and interaction ($F_{(9,1584)} = 16.73$; $P = 1.47 \times 10^{-26}$). Note that the anxiety scores of all trials were defined from other trials (i.e., we did not use them themselves in order to avoid circularity). The mean rating score for the anxiety trials was significantly higher than that for the neutral trials for all participants ($P < 0.05$ for all participants, Wilcoxon rank-sum test).

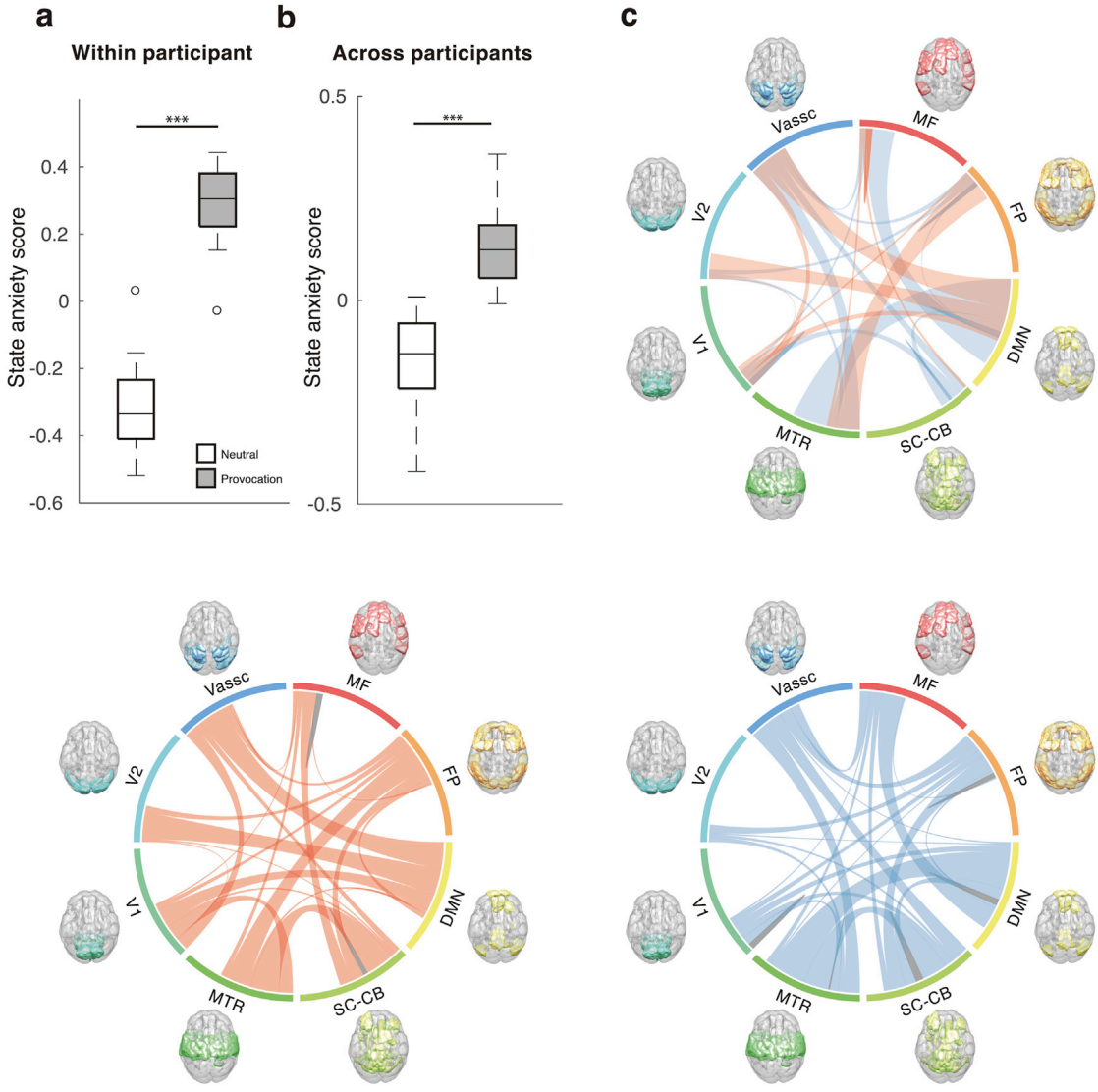

Fig. 3. State anxiety-related brain network defined by the anxiety provocation task. (**a–b**) The anxiety scores of the anxiety stimuli (gray) and neutral stimuli (white) for (**a**) within- and (**b**) across-participant analyses. For visualization purposes, the anxiety scores of each participant were normalized within each participant. Note that this normalization was not performed in any quantitative analysis. (**c**) Macroscale visualization of high-anxiety (lower left, red), low-anxiety (lower right, blue) and difference between the two (upper right, red and blue) networks for the number of FCs that consistently differed between the trials of anxiety stimuli and neutral stimuli across participants. Canonical networks include the medial frontal (MF), frontoparietal (FP), default mode network (DMN), subcortical-cerebellum (SC-CB), motor (MTR), visual I (V1), visual II (V2), and visual association (VAssc). For the plots of high-anxiety and low-anxiety networks, connection lines are colored gray within the same network and red (high) or blue (low) between two networks. For the plot of the difference between the two networks, connection lines are colored dark-red (high) or dark-blue (low) within the same network and red (high) or blue (low) between two networks. ***Two-way repeated measures ANOVA, $P < 0.001$.

Across-participant generalization

To investigate whether the brain network is different between neutral and anxious states in the same manner across participants, we expanded the previous analysis from the within-participant paradigm to the across-participant paradigm (Fig. 2b). We applied two-way repeated measures ANOVA to the anxiety scores of all trials (N = 1,585; participant × stimulus [anxiety or neutral]) and obtained similar results to the previous analysis, that is, the effect of the stimulus was significant ($F_{(1,1585)} = 22.58$; $P = 2.20 \times 10^{-6}$). Fig. 3b shows the anxiety scores of the trials of anxiety stimuli and neutral stimuli, which were normalized within participants. We also found a significant effect of participant ($F_{(9,1584)} = 20.85$; $P = 1.56 \times 10^{-33}$) but no interaction effect ($F_{(9,1584)} = 1.44$; $P = 0.17$).

Visualization of the state anxiety-related brain network

Through the leave-one-participant-out cross-validation procedure, we observed hundreds of FCs selected at all iterations, that is, hundreds of FCs consistently differed between the trials of anxiety stimuli and neutral stimuli across participants. To facilitate characterization of the biological substrates of the state anxiety-related FCs, we grouped the 268 ROIs into eight macroscale canonical networks. Fig. 3c shows the circle plot of the FCs that were involved in the high-anxiety network, low-anxiety network and the difference between the two networks. The numbers of FCs in each of the two macroscale regions (the medial frontal [MF], frontoparietal [FP], default mode network [DMN], subcortical-cerebellum [SC-CB], motor [MTR], visual I [V1], visual II [V2], and visual association [VAssc]) are presented as the thickness of the connection lines. Although the FCs in the DMN were selected to some extent, the FCs in both networks were widely distributed rather than locally constrained.

Beyond anxiety dimension generalization: resting-state fMRI from the Human Connectome Project

To investigate whether there is a common brain network between state and trait anxiety, we examined all trials of the anxiety provocation task (N = 1,585) using the anxiety score that was defined by the HCP data with the rs-fMRI and behavioral trait anxiety scale score (N = 879) (Fig. 2c). We applied a two-way repeated measures ANOVA to the anxiety scores of all trials (participant × stimulus [anxiety or neutral]) and the results showed that the anxiety scores of the trials of anxiety stimuli and neutral stimuli were significantly different ($F_{(1,1584)} = 7.5$; $P = 6.24 \times 10^{-3}$). Fig. 4a shows the normalized anxiety scores within participants. We also found a significant effect of participant ($F_{(9,1584)} = 36.9$; $P = 1.06 \times 10^{-59}$) and interaction ($F_{(9,1584)} = 3.26$; $P = 6.07 \times 10^{-4}$). Fig. 4b shows the high-anxiety, low-anxiety and the difference between the two networks in a macroscale defined by the HCP data with the rs-fMRI and behavioral trait anxiety scale score. The high- and low-anxiety networks of trait anxiety revealed more dissimilar patterns of the FCs than those of state anxiety. In particular, the FCs within the frontoparietal and medial-frontal networks and between them were frequently selected in the high-anxiety network. We also applied state anxiety brain networks to trait anxiety data. For each participant in the HCP dataset, we calculated the anxiety score, which was defined according to all trials in the anxiety provocation task. Comparison of

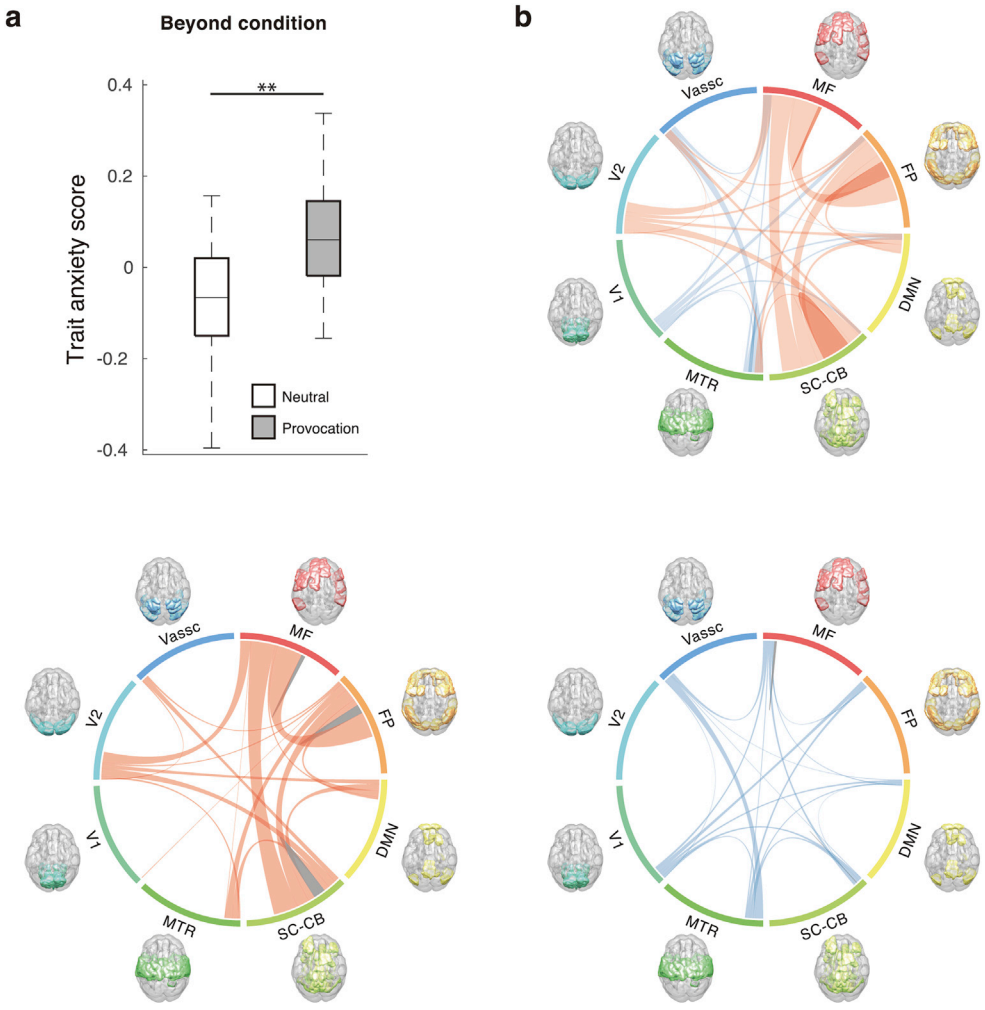

Fig. 4. Generalization to different dimensions of anxiety. (**a**) The anxiety scores of the anxiety stimuli (gray) and neutral stimuli (white). (**b**) High-anxiety (lower left, red), low-anxiety (lower right, blue) and difference between the two (upper right, red and blue) networks defined by the HCP data with the rs-fMRI and behavioral trait anxiety scale scores in a macroscale. The numbers of FCs in each of the two macroscale regions are presented as the thickness of the connection lines. For the plots of high-anxiety and low-anxiety networks, connection lines are colored gray within the same network and red (high) or blue (low) between two networks. For the plot of the difference between the two networks, connection lines are colored dark-red (high) or dark-blue (low) within the same network and red (high) or blue (low) between two networks. Abbreviations are the same as in Fig. 3. **Two-way repeated measures ANOVA, $P < 0.01$.

participants with behavioral trait anxiety scale scores above the median for the whole sample with other participants showed that the mean anxiety score of the former group was significantly larger than that of the latter group ($t_{(877)} = 2.29$, $P = 0.022$, two-sample t-test). We further calculated the correlation between the anxiety score and trait anxiety. Although the correlation was positive, it was not significant (Pearson's $R = 0.053$; $P = 0.11$). We suggest that this was because the anxiety score was derived from data categorized by two types of trial (i.e., anxiety or neutral trial), rather than from continuous data.

Common brain network between state and trait anxiety

To evaluate the degree of overlap between brain networks related to state and trait anxiety, we counted the common FCs between these two networks. Among the whole 35,778 FCs used, 13 FCs were included in the same network (the high- or low-anxiety network) in both dimensions of anxiety (state or trait anxiety) (Table 1). Specifically, when we extracted FCs using the whole dataset of state anxiety, 1.226 FCs were selected, comprising 601 FCs in the high-anxiety network and 625 FCs in the low-anxiety network. For trait anxiety, 342 FCs were selected, comprising 267 FCs in the high-anxiety network and 75 FCs in the low-anxiety network. Finally, 4 and 9 FCs overlapped in the high- and low-anxiety networks, respectively. Fig. 5a shows the spatial distribution of these 13 FCs. Two of the 4 FCs in the high-anxiety network had the orbitofrontal cortex as their node. The nodes of the other 2 FCs were the thalamus and superior temporal, and the temporal pole and primary visual cortex, respectively. In contrast, the FCs of the low-anxiety network were in the motor cortex and occipital cortex. For macroscopic interpretation, Fig. 5b shows the common FCs in a macroscale. The FCs in the high-anxiety network frequently belonged to the frontoparietal and medial-frontal network. The FCs in the low-anxiety network belonged to the default mode network, subcortical-cerebellum, and motor network. Finally, we compared 10,000 randomly generated anxiety networks with our results and found that the probability for obtaining the 13 overlapped FCs was statistically significant ($P < 0.02$). This suggests that the 13 FCs were not merely randomly overlapping but play a significant role as a common brain network of anxiety.

The common brain network of anxiety among different populations: patients with OCD from three different sites

To investigate which brain network is involved in pathological anxiety, we compared the anxiety scores defined by state anxiety and/or trait anxiety of patients with OCD and HCs from the three different datasets (N = 174) (Fig. 2d). We applied two-way repeated measures ANOVA to the anxiety scores of all trials (population [HC or OCD] × sites [site A, B, or C]). We found that only when we applied the anxiety score defined by the 13 common FCs, the anxiety scores of patients with OCD were significantly different from those of HCs (Fig. 5c; $F_{(1,173)} = 6.76$; $P = 0.01$). We also found a modest effect of site ($F_{(2,173)} = 2.63$; $P = 0.07$) but no interaction effect ($F_{(2,173)} = 0.31$; $P = 0.73$). We varied the thresholds to 0.05 and 0.1. We found that more liberal thresholds yielded a greater number of common FCs. Although the mean anxiety scores calculated by liberal thresholds were still larger for OCD patients than for HC participants, they were not generalized better to the OCD data than those using 0.01 ($P > 0.05$ for 0.5 and 0.1). In addition, the common FCs with liberal thresholds could not be used for classification ($P > 0.05$ for 0.5 and 0.1). We suggest that such lower generalizability is because of the increase of noise from FCs selected in the liberal thresholds. Notably, when we conducted the same analyses using the anxiety scores defined by either state or trait anxiety, no significant differences were observed for any comparisons ($P > 0.05$ for all comparisons). Finally, to test whether the 13 common FCs specified above could also classify participants into patients with OCD or HCs, we evaluated the performance of a classifier that was composed of these FCs. Our model, developed using the 13 common FCs, achieved a significantly higher AUC (AUC = 0.60; Sensitivity = 0.57; Specificity = 0.56) than other models that consisted of the same number of randomly selected FCs (1,000 times permutation test; $P < 0.05$). This analysis indicates that the probability of obtaining the AUC was small and demonstrates that the 13 FCs identified in the main analyses specifically contain information useful to predict OCD.

Control analyses for head motion

Researchers in the field of FC have raised substantial concerns about the effect of head motion (Ciric et al., 2017; Satterthwaite et al., 2012; van Dijk et al., 2012). Therefore, we investigated whether there was a systematic relationship between head motion and state, trait, or pathological anxiety. For each participant, we calculated the framewise displacement (FD) at each time point by summing all six motion parameters (see Supplementary Notes). In the anxiety provocation task, there was no significant difference in mean FD between conditions for 9 of the 10 participants ($t_{(124)} = 0.24$, $t_{(124)} = 1.14$, $t_{(124)} = 0.03$, $t_{(124)} = 1.70$, $t_{(124)} = 0.25$, $t_{(124)} = 0.88$, $t_{(124)} = 1.72$, $t_{(250)} = 0.76$, and $t_{(250)} = 0.67$, respectively. $P > 0.05$ for all participants, two-sample t-test). For the remaining participant, the mean FD for the anxiety trials was significantly larger than for the neutral trials ($t_{(250)} = 3.30$, $P = 0.001$, two-sample t-test). For 4 of the 10 participants, the mean FD for the neutral trials was larger than for the anxiety trials (although this difference was not statistically significant). These results suggest that there was no systematic motion-related bias in the anxiety provocation task. For the HCP data, mean FD was not significantly correlated with the behavioral trait anxiety scale (Pearson's $R = 0.037$; $P = 0.28$). For the OCD data, there was no significant difference in mean FD between OCD and HC for site A ($t_{(106)} = 1.73$, $P > 0.08$, two-sample t-test) and site B ($t_{(26)} = 0.26$, $P > 0.79$, two-sample t-test) among the three sites. For site C, the mean FD of the OCD participants was significantly larger than that of the HC participants ($t_{(36)} = 2.72$, $P = 0.01$, two-sample t-test).

Table 1
Properties of the 13 common FCs between state and trait anxiety. Mid, Middle; Sup, Superior; Inf, Inferior; Orb, Orbitofrontal; SMA, Supplemental Motor Area; R, Right; L, Left.

ID	Anxiety network	Terminal regions			
		Region 1 (AAL)	Functional network	Region 2 (AAL)	Functional network
1	High	Frontal_Sup_L	Medial frontal	Frontal_Sup_Orb_R	Frontoparietal
2	High	Angular_L	Frontoparietal	Frontal_Sup_Orb_R	Frontoparietal
3	High	Thalamus_R	Subcortical-cerebellum	Temporal_Mid_R	Medial frontal
4	High	Occipital_Inf_L	Visual II	Temporal_Pole_Mid_L	Medial frontal
5	Low	Temporal_Mid_R	Visual association	Precentral_R	Motor
6	Low	SMA_L	Medial frontal	Parietal_Sup_R	Visual association
7	Low	Occipital_Mid_R	Default mode	SupraMarginal_R	Motor
8	Low	SMA_L	Medial frontal	Occipital_Mid_R	Default mode
9	Low	Postcentral_L	Motor	Occipital_Mid_R	Default mode
10	Low	Parietal_Inf_L	Motor	Occipital_Mid_R	Default mode
11	Low	SupraMarginal_L	Motor	Hippocampus_R	Subcortical-cerebellum
12	Low	Postcentral_L	Motor	Temporal_Mid_R	Visual association
13	Low	Paracentral_Lobule_L	Motor	Temporal_Mid_R	Visual association

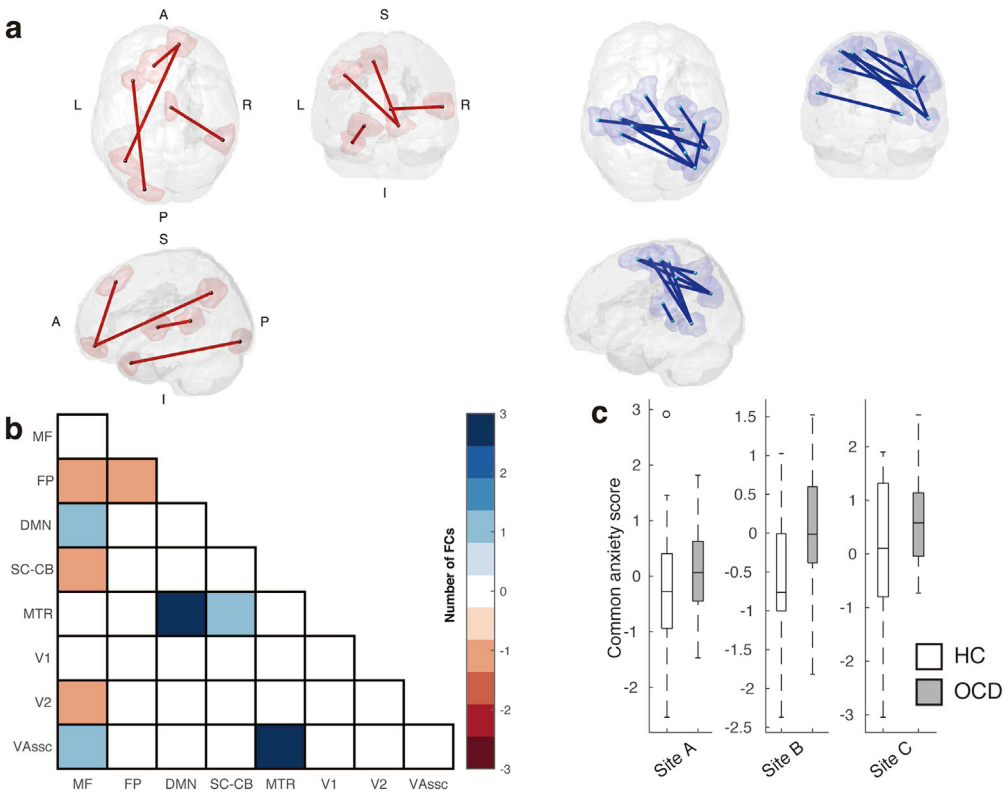

Fig. 5. The common brain network and its generalization to patients with obsessive-compulsive disorder at the three different sites. (**a**) Spatial distribution of the 13 common FCs. (**b**) Matrix for the number of FCs between each pair of canonical networks in the high-anxiety (red) and low-anxiety (blue) networks. Abbreviations are the same as in Fig. 3. (**c**) The anxiety scores of the healthy controls (white) and patients with OCD (gray) for each site. A, anterior; P, posterior; R, right; L, left; S, superior; I, inferior.

However, the mean FD of the HC participants was larger than that of the OCD participants for site B (although this difference was not statistically significant). Furthermore, all three sites showed the same trend as shown for anxiety scores (see Fig. 5c). These results suggest that there were no systematic effects of head motion.

Discussion

In this study, we have characterized a common brain network among state, trait, and pathological anxiety by analyzing different fMRI datasets that were bound to different dimensions of anxiety in a data-driven manner. We first demonstrated that there was a common brain network of state anxiety within and between participants. We then demonstrated that the trait anxiety-related brain network, defined by rs-fMRI with the behavioral trait anxiety scale score, can be generalized to state anxiety. Finally, we found that we could characterize pathological anxiety, as represented by patients with OCD, by using the common FCs between state and trait anxiety.

Although previous fMRI studies have reported patterns of neural activation during anxiety provocation tasks (Blair et al., 2008; Lorberbaum et al., 2004; Mataix-Cols et al., 2003; Nakao et al., 2005; Tillfors et al., 2001), they did not investigate whole-brain FCs and did not perform cross-validation. In the present study, we first demonstrated that the common FCs related to state anxiety across participants can be detected in a fully cross-validated manner. These results suggest that when we feel anxiety in our daily life, common brain regions might be co-activated within and between individuals. It should be noted that in the main analyses, we found interaction effects in the within-participant anxiety detection and beyond anxiety dimension generalization, but no interaction in the across-participant generalization. For the first two analyses, some participants showed more pronounced differences between anxiety and neutral blocks than others. However, we found no such evidence for across-participant generalization (see Supplementary Notes). We suggest that one reason for this difference is the larger sample size of the across-participant analysis compared with the other two analyses. We also suggest that the increase in variability among trials might have contributed to a decrease in the variability in generalization.

Our findings also revealed that there is a common brain network between state and trait anxiety. Our results suggest that the resting-state FC patterns of participants who tend to feel anxiety in their daily life is similar to the FC pattern during evoked anxiety. This finding is noteworthy because previous studies showed that state and trait anxiety often interact (Mathews, 1990; Williams et al., 1996). In these studies, the authors hypothesized that participants with high trait anxiety become increasingly vigilant under stress, further increasing their anxiety level. In contrast, participants with low trait anxiety show a defensive response under stress, serving to restrain further anxiety increases. Common FCs may contribute to this positive-negative feedback loop of anxiety.

In the present study, we identified common FCs between state and trait anxiety, and the number of common FCs was significantly larger than in randomly selected cases. Furthermore, although we employed a fully data-driven approach rather than setting an a priori hypothesis, the pattern of FCs revealed was highly meaningful. That is, frontal and default mode networks were more likely chosen, and they were often reported in previous studies as anxiety-related regions (Beucke et al., 2013; Liao et al., 2010; Liu et al., 2015; Modi et al., 2015; Tian et al., 2016; Wang et al., 2016; Yin et al., 2016). More specifically, the orbitofrontal cortex, thalamus, and cingulate cortex were included in the high-anxiety network and the default mode network was included in the low-anxiety network. The increased and decreased FCs in these areas for state, trait, and pathological anxiety have frequently been reported. It should be noted that, as shown in several seed-based studies, the amygdala has often been reported as a central region of anxiety (Banca et al., 2015; Baur et al., 2013; Cha et al., 2014; Hahn et al., 2011; Kim et al., 2011). In the present study, we found no evidence indicating that the amygdala is fundamentally involved in anxiety, as operationalized here. Intriguingly, the above studies using data-driven procedures commonly do not report the amygdala and, additionally, most have reported a frontal and/or default mode network. To our knowledge, no data-driven study of anxiety has investigated the generalizable FCs

among different dimensions of anxiety. Our study has quantitatively evaluated the relative importance of the conventionally investigated brain regions to whole brain using a fully data-driven approach.

When we used the common FCs between state and trait anxiety to calculate the anxiety scores of patients with OCD and HCs, patients with OCD showed higher anxiety scores than HCs. Furthermore, the FCs could classify whole participants into HCs and patients with OCD in a fully cross-validated manner. However, we could not find such results when we used anxiety scores defined by either state or trait anxiety data. Our findings thus demonstrate that the common FCs between state and trait anxiety are key components of pathological anxiety. Our findings may also be theoretically helpful for constructing a biologically validated model of anxiety that explicitly considers the interaction among state, trait, and pathological anxiety. In addition, future work should also investigate the causal interaction among state, trait, and pathological anxiety by modulating the brain network, for example, via neurofeedback (Megumi et al., 2015), to obtain a deeper understanding of the neural mechanism of anxiety. Our findings may contribute to the identification of a reasonable target for intervention.

The present study focused on anxiety that is typically defined as a state that can be induced by abstract threats that may happen in the future (Calhoon and Tye, 2015). This type of anxiety is considered to be a central component of some psychiatric disorders. For example, OCD is one such disorder, and patients with OCD cannot avoid impulsively reacting to relieve anxious feelings. However, there is another type of anxiety that is induced by more direct, predictable threat. This type of anxiety is also considered a central component of other psychiatric disorders. Whether there is an interaction or overlap between these anxiety types in the brain remains unknown, and future studies should investigate this by applying our neural marker to patients with other psychiatric disorders. It should also be noted that in the anxiety provocation task, we recruited individuals who tended to feel anxiety related to OCD in their daily life; this may have induced a bias for extracting a state anxiety brain network. We recruited anxious individuals for the following reasons. First, such individuals are sensitive to anxiety-provoking stimuli and can effectively induce their own state anxiety during fMRI. This was crucial, because we had a limited number of trials in the fMRI experiments. Second, we extracted the state anxiety-related network by comparing two within-participant states: a neutral state and an anxiety state. This procedure should have helped to exclude brain networks that contribute only to trait anxiety. Third, the trait anxiety dataset (HCP) was not related to specific psychiatric disorders and the participants of the anxiety provocation task had no psychiatric disorder diagnoses. It is thus not obvious that only an anxiety brain network common to state and trait anxiety could generalize to the OCD dataset. However, future studies should address this issue by conducting similar experiments with healthy people with lower trait anxiety.

Conclusion

In this study, we found a common brain network of anxiety among state, trait, and pathological anxiety. These results provide direct evidence that different dimensions of anxiety have a substantial biological inter-relationship. Our results also have the potential to be used for the treatment evaluation. Furthermore, given that the hypothesis of a psychiatric disorder spectrum is gaining attention, our results may promote further investigation of various human characteristics, including psychiatric disorder, from the perspective of anxiety.

Acknowledgements

This research was conducted as the “Application of DecNef for development of diagnostic and cure system for mental disorders and construction of clinical application bases” of the Strategic Research Program for Brain Sciences from the Japan Agency for Medical Research and Development, AMED. This work was partly supported by JSPS KAKENHI Grant Number 25119001, the Joint Usage/Research Center at ISER, Osaka University, and a grant from the Carlos III Health Institute (PI13/01958). Dr. Soriano-Mas is funded by a Miguel Servet contract from the Carlos III Health Institute (CPII16/00048). Data were provided [in part] by the Human Connectome Project, WU-Minn Consortium (Principal Investigators: David Van Essen and Kamil Ugurbil; 1U54MH091657) funded by the 16 NIH Institutes and Centers that support the NIH Blueprint for Neuroscience Research; and by the McDonnell Center for Systems Neuroscience at Washington University. We thank O. Yamashita, H. Imamizu, B. Seymour and W. Yoshida for helpful discussions and proofreading the manuscript. We thank T. Okada, H. Ito, and the technical engineers for their assistance in MRI data acquisition. We thank K. Tamura, S. Kimura, and K. Inoue for their assistance in the assessment of patients. We thank N. Izumihara for his support for visualization.

Appendix A. Supplementary data

Supplementary data related to this article can be found at https://doi.org/10.1016/j.neuroimage.2018.01.080.

References

Adam, D., 2013. On the spectrum. Nature 496, 6–8. https://doi.org/10.1038/496416a.

Banca, P., Voon, V., Vestergaard, M.D., Philipiak, G., Almeida, I., Pocinho, F., Relvas, J., Castelo-Branco, M., 2015. Imbalance in habitual versus goal directed neural systems during symptom provocation in obsessive-compulsive disorder. Brain 138, 798–811. https://doi.org/10.1093/brain/awu379.

Baur, V., Hänggi, J., Langer, N., Jäncke, L., 2013. Resting-state functional and structural connectivity within an insula-amygdala route specifically index state and trait anxiety. Biol. Psychiatr. 73, 85–92. https://doi.org/10.1016/j.biopsych.2012.06.003.

Beucke, J.C., Sepulcre, J., Talukdar, T., Linnman, C., Zschenderlein, K., Endrass, T., Kaufmann, C., Kathmann, N., 2013. Abnormally high degree connectivity of the orbitofrontal cortex in obsessive-compulsive disorder. JAMA psychiatry 70, 619–629. https://doi.org/10.1001/jamapsychiatry.2013.173.

Blair, K., Geraci, M., Devido, J., McCaffrey, D., Chen, G., Vythilingam, M., Ng, P., Hollon, N., Jones, M., Blair, R.J.R., Pine, D.S., 2008. Neural response to self- and other referential praise and criticism in generalized social phobia. Arch. Gen. Psychiatr. 65, 1176–1184. https://doi.org/10.1001/archpsyc.65.10.1176.

Burns, G.L., Keortge, S.G., Formea, G.M., Sternberger, L.G., 1996. Revision of the Padua Inventory of obsessive compulsive disorder symptoms: distinctions between worry, obsessions, and compulsions. Behav. Res. Ther. 34, 163–173.

Calhoon, G.G., Tye, K.M., 2015. Resolving the neural circuits of anxiety. Nat. Neurosci. 18, 1394–1404. https://doi.org/10.1038/nn.4101.

Cha, J., Greenberg, T., Carlson, J.M., Dedora, D.J., Hajcak, G., Mujica-Parodi, L.R., 2014. Circuit-wide structural and functional measures predict ventromedial prefrontal cortex fear generalization: implications for generalized anxiety disorder. J. Neurosci. 34, 4043–4053. https://doi.org/10.1523/JNEUROSCI.3372-13.2014.

Ciric, R., Wolf, D.H., Power, J.D., Roalf, D.R., Baum, G.L., Ruparel, K., Shinohara, R.T., Elliott, M.A., Eickhoff, S.B., Davatzikos, C., Gur, R.C., Gur, R.E., Bassett, D.S., Satterthwaite, T.D., 2017. Benchmarking of participant-level confound regression strategies for the control of motion artifact in studies of functional connectivity. Neuroimage 154, 174–187. https://doi.org/10.1016/j.neuroimage.2017.03.020.

Cole, M.W., Yarkoni, T., Repovš, G., Anticevic, A., Braver, T.S., 2012. Global connectivity of prefrontal cortex predicts cognitive control and intelligence. J. Neurosci. 32, 8988–8999. https://doi.org/10.1523/JNEUROSCI.0536-12.2012.

Deichmann, R., Gottfried, J., Hutton, C., Turner, R., 2003. Optimized EPI for fMRI studies of the orbitofrontal cortex. Neuroimage 19, 430–441. https://doi.org/10.1016/S1053-8119(03)00073-9.

Etkin, A., Prater, K.E., Hoeft, F., Menon, V., Schatzberg, A.F., 2010. Failure of anterior cingulate activation and connectivity with the amygdala during implicit regulation of emotional processing in generalized anxiety disorder. Am. J. Psychiatr. 167, 545–554. https://doi.org/10.1176/appi.ajp.2009.09070931.

Finn, E.S., Shen, X., Scheinost, D., Rosenberg, M.D., Huang, J., Chun, M.M., Papademetris, X., Todd Constable, R., 2015. Functional connectome fingerprinting: identifying individuals using patterns of brain connectivity. Nat. Neurosci. 18, 1–11. https://doi.org/10.1038/nn.4135.

First, M.B., Spitzer, R.L., Gibbon, M., Williams, J.B.W., 2002. Structured Clinical Interview for DSM-IV-TR Axis I Disorders. Research Version, Non-patient Edition. (SCID-I/NP). Biometrics Research Department. New York State Psychiatric Institute, New York.

Fox, M.D., Greicius, M., 2010. Clinical applications of resting state functional connectivity. Front. Syst. Neurosci. 4, 19. https://doi.org/10.3389/fnsys.2010.00019.

Giménez, M., Pujol, J., Ortiz, H., Soriano-Mas, C., López-Solà, M., Farré, M., Deus, J., Merlo-Pich, E., Martín-Santos, R., 2012. Altered brain functional connectivity in relation to perception of scrutiny in social anxiety disorder. Psychiatry Res. Neuroimaging. 202, 214–223. https://doi.org/10.1016/j.pscychresns.2011.10.008.

Gonzalez-Castillo, J., Hoy, C.W., Handwerker, D. a., Robinson, M.E., Buchanan, L.C., Saad, Z.S., Bandettini, P. a., 2015. Tracking ongoing cognition in individuals using brief, whole-brain functional connectivity patterns. Proc. Natl. Acad. Sci. Unit. States Am. 112, 8762–8767. https://doi.org/10.1073/pnas.1501242112.

Greenberg, P.E., Sisitsky, T., Kessler, R.C., Finkelstein, S.N., Berndt, E.R., Davidson, J.R.T., Ballenger, J.C., Fyer, A.J., 1999. The economic burden of anxiety disorders in the 1990s. J. Clin. Psychiatr. 60, 427–435. https://doi.org/10.4088/JCP.v60n0702.

Griffanti, L., Salimi-Khorshidi, G., Beckmann, C.F., Auerbach, E.J., Douaud, G., Sexton, C.E., Zsoldos, E., Ebmeier, K.P., Filippini, N., Mackay, C.E., Moeller, S., Xu, J., Yacoub, E., Baselli, G., Ugurbil, K., Miller, K.L., Smith, S.M., 2014. ICA-based artefact removal and accelerated fMRI acquisition for improved resting state network imaging. Neuroimage 95, 232–247. https://doi.org/10.1016/j.neuroimage.2014.03.034.

Gruner, P., Vo, A., Argyelan, M., Ikuta, T., Degnan, A.J., John, M., Peters, B.D., Malhotra, A.K., Uluğ, A.M., Szeszko, P.R., 2014. Independent component analysis of resting state activity in pediatric obsessive-compulsive disorder. Hum. Brain Mapp. 35, 5306–5315. https://doi.org/10.1002/hbm.22551.

Hahn, A., Stein, P., Windischberger, C., Weissenbacher, A., Spindelegger, C., Moser, E., Kasper, S., Lanzenberger, R., 2011. Reduced resting-state functional connectivity between amygdala and orbitofrontal cortex in social anxiety disorder. Neuroimage 56, 881–889. https://doi.org/10.1016/j.neuroimage.2011.02.064.

Harrison, B.J., Soriano-Mas, C., Pujol, J., Ortiz, H., López-Solà, M., Hernández-Ribas, R., Deus, J., Alonso, P., Yücel, M., Pantelis, C., Menchon, J.M., Cardoner, N., 2009. Altered corticostriatal functional connectivity in obsessive-compulsive disorder. Arch. Gen. Psychiatr. 66, 1189–1200. https://doi.org/10.1001/archgenpsychiatry.2009.152.

Hodgson, R.J., Rachman, S., 1977. Obsessional-compulsive complaints. Behav. Res. Ther. 15, 389–395.

Hu, X., Liu, Q., Li, B., Tang, W., Sun, H., Li, F., Yang, Y., Gong, Q., Huang, X., 2016. Multivariate pattern analysis of obsessive-compulsive disorder using structural neuroanatomy. Eur. Neuropsychopharmacol 26, 246–254. https://doi.org/10.1016/j.euroneuro.2015.12.014.

Kessler, R.C., Berglund, P., Demler, O., Jin, R., Merikangas, K.R., Walters, E.E., 2005. Lifetime prevalence and age-of-onset distributions of. Arch. Gen. Psychiatr. 62, 593–602. https://doi.org/10.1001/archpsyc.62.6.593.

Kim, M.J., Gee, D.G., Loucks, R.A., Davis, F.C., Whalen, P.J., 2011. Anxiety Dissociates dorsal and ventral medial prefrontal cortex functional connectivity with the amygdala at rest. Cerebr. Cortex 21, 1667–1673. https://doi.org/10.1093/cercor/bhq237.

Li, F., Huang, X., Tang, W., Yang, Y., Li, B., Kemp, G.J., Mechelli, A., Gong, Q., 2014. Multivariate pattern analysis of DTI reveals differential white matter in individuals with obsessive-compulsive disorder. Hum. Brain Mapp. 35, 2643–2651. https://doi.org/10.1002/hbm.22357.

Liao, W., Chen, H., Feng, Y., Mantini, D., Gentili, C., Pan, Z., Ding, J., Duan, X., Qiu, C., Lui, S., Gong, Q., Zhang, W., 2010. Selective aberrant functional connectivity of resting state networks in social anxiety disorder. Neuroimage 52, 1549–1558. https://doi.org/10.1016/j.neuroimage.2010.05.010.

Liem, F., Varoquaux, G., Kynast, J., Beyer, F., Masouleh, S.K., Huntenburg, J.M., Lampe, L., Rahim, M., Abraham, A., Craddock, R.C., Riedel-Heller, S., Luck, T., Loeffler, M., Schroeter, M.L., Witte, A.V., Margulies, D.S., 2016. Predicting brain-age from multimodal imaging data captures cognitive impairment. Neuroimage. https://doi.org/10.1016/j.neuroimage.2016.11.005.

Liu, F., Zhu, C., Wang, Y., Guo, W., Li, M., Wang, W., Long, Z., Meng, Y., Cui, Q., Zeng, L., Gong, Q., Zhang, W., Chen, H., 2015. Disrupted cortical hubs in functional brain networks in social anxiety disorder. Clin. Neurophysiol. 126, 1711–1716. https://doi.org/10.1016/j.clinph.2014.11.014.

Lorberbaum, J.P., Kose, S., Johnson, M.R., Arana, G.W., Sullivan, L.K., Hamner, M.B., Ballenger, J.C., Lydiard, R.B., Brodrick, P.S., Bohning, D.E., George, M.S., 2004. Neural correlates of speech anticipatory anxiety in generalized social phobia. Neuroreport 15, 2701–2705 doi: 00001756-200412220-00003 [pii].

Mataix-Cols, D., Cullen, S., Lange, K., Zelaya, F., Andrew, C., Amaro, E., Brammer, M.J., Williams, S.C., Speckens, A., Phillips, M.L., 2003. Neural correlates of anxiety associated with obsessive-compulsive symptom dimensions in normal volunteers. Biol. Psychiatr. 53, 482–493. https://doi.org/10.1016/S0006-3223(02)01504-4.

Mathews, A., 1990. Why worry? The cognitive function of anxiety. Behav. Res. Ther. 28, 455–468. https://doi.org/10.1016/0005-7967(90)90132-3.

Megumi, F., Yamashita, A., Kawato, M., Imamizu, H., 2015. Functional MRI neurofeedback training on connectivity between two regions induces long-lasting changes in intrinsic functional network. Front. Hum. Neurosci. 9, 160. https://doi.org/10.3389/fnhum.2015.00160.

Modi, S., Kumar, M., Kumar, P., Khushu, S., 2015. Aberrant functional connectivity of resting state networks associated with trait anxiety. Psychiatry Res. Neuroimaging. 234, 25–34. https://doi.org/10.1016/j.pscychresns.2015.07.006.

Nakao, T., Nakagawa, A., Yoshiura, T., Nakatani, E., Nabeyama, M., Yoshizato, C., Kudoh, A., Tada, K., Yoshioka, K., Kawamoto, M., Togao, O., Kanba, S., 2005. Brain activation of patients with obsessive-compulsive disorder during neuropsychological and symptom provocation tasks before and after symptom improvement: a functional magnetic resonance imaging study. Biol. Psychiatr. 57, 901–910. https://doi.org/10.1016/j.biopsych.2004.12.039.

Pilkonis, P.A., Choi, S.W., Reise, S.P., Stover, A.M., Riley, W.T., Cella, D., 2011. Item banks for measuring emotional distress from the patient-reported outcomes measurement information system (PROMIS): depression, anxiety, and anger. Assessment 18, 263–283. https://doi.org/10.1177/1073191111411667.

Power, J.D., Barnes, K.A., Snyder, A.Z., Schlaggar, B.L., Petersen, S.E., 2012. Spurious but systematic correlations in functional connectivity MRI networks arise from subject motion. Neuroimage 59, 2142–2154. https://doi.org/10.1016/j.neuroimage.2011.10.018.

Rosenberg, M.D., Finn, E.S., Scheinost, D., Papademetris, X., Shen, X., Constable, R.T., Chun, M.M., 2016. A neuromarker of sustained attention from whole-brain functional connectivity. Nat. Neurosci. 19, 165–171. https://doi.org/10.1038/nn.4179.

Rotge, J.-Y., Guehl, D., Dilharreguy, B., Cuny, E., Tignol, J., Bioulac, B., Allard, M., Burbaud, P., Aouizerate, B., 2008. Provocation of obsessive-compulsive symptoms: a quantitative voxel-based meta-analysis of functional neuroimaging studies. J. Psychiatry Neurosci. 33, 405–412.

Sakai, Y., Narumoto, J., Nishida, S., Nakamae, T., Yamada, K., Nishimura, T., Fukui, K., 2011. Corticostriatal functional connectivity in non-medicated patients with obsessive-compulsive disorder. Eur. Psychiatr. 26, 463–469. https://doi.org/10.1016/j.eurpsy.2010.09.005.

Salimi-Khorshidi, G., Douaud, G., Beckmann, C.F., Glasser, M.F., Griffanti, L., Smith, S.M., 2014. Automatic denoising of functional MRI data: combining independent component analysis and hierarchical fusion of classifiers. Neuroimage 90, 449–468. https://doi.org/10.1016/j.neuroimage.2013.11.046.

Satpute, A.B., Mumford, J.A., Naliboff, B.D., Poldrack, R.A., 2012. Human anterior and posterior hippocampus respond distinctly to state and trait anxiety. Emotion 12, 58–68. https://doi.org/10.1037/a0026517.

Satterthwaite, T.D., Wolf, D.H., Loughead, J., Ruparel, K., Elliott, M.A., Hakonarson, H., Gur, R.C., Gur, R.E., 2012. Impact of in-scanner head motion on multiple measures of functional connectivity: relevance for studies of neurodevelopment in youth. Neuroimage 60, 623–632. https://doi.org/10.1016/j.neuroimage.2011.12.063.

Shen, X., Finn, E.S., Scheinost, D., Rosenberg, M.D., Chun, M.M., Papademetris, X., Constable, R.T., 2017. Using connectome-based predictive modeling to predict individual behavior from brain connectivity. Nat. Protoc. 12, 506–518. https://doi.org/10.1038/nprot.2016.178.

Soriano-Mas, C., Pujol, J., Alonso, P., Cardoner, N., Menchón, J.M., Harrison, B.J., Deus, J., Vallejo, J., Gaser, C., 2007. Identifying patients with obsessive-compulsive disorder using whole-brain anatomy. Neuroimage 35, 1028–1037. https://doi.org/10.1016/j.neuroimage.2007.01.011.

Takagi, Y., Sakai, Y., Lisi, G., Yahata, N., Abe, Y., Nishida, S., Nakamae, T., Morimoto, J., Kawato, M., Narumoto, J., Tanaka, S.C., 2017. A neural marker of obsessive-compulsive disorder from whole-brain functional connectivity. Sci. Rep. 7, 7538.

Tian, X., Wei, D., Du, X., Wang, K., Yang, J., Liu, W., Meng, J., Liu, H., Liu, G., Qiu, J., 2016. Assessment of trait anxiety and prediction of changes in state anxiety using functional brain imaging: a test-retest study. Neuroimage 133, 408–416. https://doi.org/10.1016/j.neuroimage.2016.03.024.

Tillfors, M., Furmark, T., Marteinsdottir, I., Fischer, H., Pissiota, A., Langstroem, B., Fredrikson, M., 2001. Cerebral blood flow in subject with social phobia during stressful speaking tasks: a PET study. Am. J. Psychiatr. 158, 1220–1226. https://doi.org/10.1176/appi.ajp.158.8.1220.

van Dijk, K.R.A., Sabuncu, M.R., Buckner, R.L., 2012. The influence of head motion on intrinsic functional connectivity MRI. Neuroimage 59, 431–438. https://doi.org/10.1016/j.neuroimage.2011.07.044.

Van Essen, D.C., Ugurbil, K., Auerbach, E., Barch, D., Behrens, T.E.J., Bucholz, R., Chang, A., Chen, L., Corbetta, M., Curtiss, S.W., Della Penna, S., Feinberg, D., Glasser, M.F., Harel, N., Heath, A.C., Larson-Prior, L., Marcus, D., Michalareas, G., Moeller, S., Oostenveld, R., Petersen, S.E., Prior, F., Schlaggar, B.L., Smith, S.M., Snyder, A.Z., Xu, J., Yacoub, E., 2012. The Human Connectome Project: a data acquisition perspective. Neuroimage 62, 2222–2231. https://doi.org/10.1016/j.neuroimage.2012.02.018.

Wang, W., Hou, J., Qian, S., Liu, K., Li, B., Li, M., Peng, Z., Xin, K., Sun, G., 2016. Aberrant regional neural fluctuations and functional connectivity in generalized anxiety disorder revealed by resting-state functional magnetic resonance imaging. Neurosci. Lett. 624, 78–84. https://doi.org/10.1016/j.neulet.2016.05.005.

Weygandt, M., Blecker, C.R., Schäfer, A., Hackmack, K., Haynes, J.D., Vaitl, D., Stark, R., Schienle, A., 2012. FMRI pattern recognition in obsessive-compulsive disorder. Neuroimage 60, 1186–1193. https://doi.org/10.1016/j.neuroimage.2012.01.064.

Williams, J.M.G., Mathews, A., MacLeod, C., 1996. The emotional Stroop task and psychopathology. Psychol. Bull. 120, 3–24. https://doi.org/10.1037/0033-2909.120.1.3.

Yamashita, O., Sato, M., Yoshioka, T., Tong, F., Kamitani, Y., 2008. Sparse estimation automatically selects voxels relevant for the decoding of fMRI activity patterns. Neuroimage 42, 1414–1429. https://doi.org/10.1016/j.neuroimage.2008.05.050.

Yin, P., Zhang, M., Hou, X., Tan, Y., Fu, Y., Qiu, J., 2016. The brain structure and spontaneous activity baseline of the behavioral bias in trait anxiety. Behav. Brain Res. 312, 355–361. https://doi.org/10.1016/j.bbr.2016.06.036.